Highly flexible and optical transparent 6F-PI/TiO_2 optical hybrid films with tunable refractive index and excellent thermal stability†

Guey-Sheng Liou,*[a] Po-Han Lin,[a] Hung-Ju Yen,[a] Yang-Yen Yu,[b] Tsung-Wei Tsai[b] and Wen-Chang Chen[ac]

Received 13th August 2009, Accepted 8th October 2009
First published as an Advance Article on the web 12th November 2009
DOI: 10.1039/b916758g

In this study, a synthesis route was developed for preparing highly transparent novel polyimide-nanocrystalline-titania hybrid optical films with a relatively high titania content (up to 50 wt%) and thickness (20–30 μm) from a soluble polyimide 6F-poly(*p*-hydroxy-imide) (**6FPI**). It has been demonstrated that the introduction of bulky CF_3 groups into polyimide backbones enhanced both solubility and optical transparency. Furthermore, the attachment of hydroxyl groups provided the organic–inorganic bonding and resulted in homogeneous hybrid solutions by controlling the mole ratio of titanium butoxide : hydroxyl groups. AFM, SEM, TEM, and XRD results indicated the formation of well-dispersed nanocrystalline-titania. The flexible hybrid films revealed excellent optical transparency in the visible range, good surface planarity, high thermally dimensional stability, and tunable refractive index. A three-layer anti-reflection coating based on the hybrid films was prepared and revealed a reflectance of less than 0.7% in the visible range, indicating its potential optical applications.

Introduction

Polymer–inorganic hybrid materials have recently attracted considerable interest owing to their enhanced mechanical, thermal, magnetic, optical, electronic, and optoelectronic properties when compared to the corresponding individual polymer or inorganic component.[1–3] Chemical methods based on *in situ* sol–gel hybridization approach made it possible to manipulate the organic–inorganic interfacial interactions at various molecular and nanometre length scales, resulting in homogeneous structures and thus overcoming the problem of nanoparticle agglomeration. For optical applications of these hybrid materials, such as high refractive index materials, optical waveguides, and anti-reflective films, the inorganic domains must be less than 40 nm to avoid scattering loss and retain the optical transparency.[4] Well-controlled morphology and phase separation were important in the preparation of transparent hybrid films, and the sol–gel reaction was widely used for making transition metal oxide solids with fine-scale microstructures. Particle sizes of less than a couple of nanometres could easily be achieved in the derived gels, and microstructural dimensions also could be maintained when subsequently crystallized at elevated temperatures.

Polymer–titania hybrid materials have been extensively investigated as high refractive index materials, including poly (methyl methacrylate) (PMMA),[5] polyimide (PI),[6,7] and others.[8] Unfortunately, the poor thermal stability of PMMA limited their device applications, which might be overcome by using thermally stable polyimide as the organic moieties. Recently, the Ueda laboratory has successfully prepared a PI-TiO_2 hybrid film containing 45 wt% silica-modified anatase-type TiO_2 nanoparticles with a refractive index of 1.81 at 632.8 nm.[9] Moreover, in order to control the titania domain size, the combination of *in situ* sol–gel processing with polymer molecular weight, coupling agent (such as 3-aminopropyl trimethoxysilane) or chelating agent (such as acetylacetone) was commonly employed to prepare the hybrid materials.[6] However, using lower molecular weight polymers and additional coupling or chelating agents to prepare the hybrid materials might affect the thermal, mechanical, and optical properties. Furthermore, PI-TiO_2 hybrid thick film with high titania content could not be achieved.

In this contribution, a new synthesis route was developed to obtain aromatic polyimide–nanocrystalline titania hybrid thick films (up to 30 μm) with tunable titania contents, refractive index, and highly optical transparency. The high weight-average molecular weight and organo-soluble polyimide with hydroxyl groups (**6FPI**) derived from 2,2-bis(3-amino-4-hydroxyphenyl)hexafluoropropane and 4,4′-oxydiphthalic dianhydride was used to prepare the titania hybrid materials. The lateral hydroxyl groups in polyimide chains could provide organic–inorganic bonding with titanium butoxide ($Ti(OBu)_4$), and highly homogeneous hybrid films with different titania contents could be successfully obtained. AFM, SEM, TEM, and XRD were used to characterize the morphologies of the resulting hybrid materials. The thermal properties, optical transmittance, and refractive index dispersion of these hybrid films were also investigated and described herein.

[a]*Institute of Polymer Science and Engineering, National Taiwan University, 1 Roosevelt Road, 4th Section, Taipei 10617, Taiwan. E-mail: gsliou@ntu.edu.tw*
[b]*Department of Materials Engineering, Mingchi University of Technology, 84 Gungjuan Road, Taishan, Taipei 243, Taiwan*
[c]*Department of Chemical Engineering, National Taiwan University, 1 Roosevelt Road, 4th Section, Taipei 10617, Taiwan*

† Electronic supplementary information (ESI) available: Proposed reaction scheme for thermal conversion, FTIR spectra of **6FPI** and **6TP50**, TGA thermograms of **6FPI** hybrid materials, TMA curve of **6TP30**, variation of the extinction coefficients; tables of inherent viscosity, molecular weights and solubility behavior of polyimide **6FPI**, and color coordinates and cutoff wavelength of **6FPI** hybrid materials. See DOI: 10.1039/b916758g

Experimental section

Materials

2,2-Bis(3-amino-4-hydroxyphenyl)hexafluoropropane (**6F-OH diamine**) (mp: 249 °C) was purchased from TCI and recrystallized from methanol. Commercially available aromatic tetracarboxylic dianhydride 4,4′-oxydiphthalic dianhydride (**OPDA**) (TCI) was purified by vacuum sublimation. The organosoluble polyimide 6F-poly(*p*-hydroxy-imide) (**6FPI**)[10] was synthesized by one-step polycondensation from **6F-OH diamine** and **ODPA** in *m*-cresol with a catalytic amount of isoquinoline at 200 °C according to a previously reported procedure. All other reagents were used as received from commercial sources.

Preparation of polyimide–titania hybrid films

The synthesis of polyimide–titania hybrid **6TP50** was used as an example to illustrate the general synthesis route used to produce the hybrid **6TPX**. Firstly, 0.12 g (0.18 mmole) of **6FPI** was dissolved in 6.0 ml of DMAc, and then 0.20 ml of HCl (37 wt%) was added very slowly into the polyimide solution and further stirred at room temperature for 30 min. Then, 0.50 ml (1.46 mmole) of $Ti(OBu)_4$ dissolved in 0.50 ml of butanol was added drop-wise into the above solution by a syringe, and then stirred at room temperature for 30 min. Finally, the resulting precursor solution of **6TP50** was filtered through a 0.45 μm PTFE filter and poured into a 6 cm glass Petri dish. The hybrid optical film could be obtained by subsequent heating program at 60 °C for 4 h, 150 °C for 3 h, and then 350 °C for 2 h under vacuum condition. After the curing process, hybrid films were immersed into water to peel off from the glass substrates and dried in vacuum. The obtained hybrid films were about 20–25 μm in thickness. For thin film preparation, the above precursor solution was diluted by DMAc and cast onto glass plate. On the other hand, the preparation of the titania film (**TP100**) was similar to the previous reported.[7]

Measurements

Fourier transform infrared (FT-IR) spectra were recorded on a PerkinElmer Spectrum 100 Model FT-IR spectrometer. The inherent viscosities were determined at 0.5 g/dL concentration using Tamson TV-2000 viscometer at 30 °C. Gel permeation chromatographic (GPC) analysis was performed on a Lab Alliance RI2000 instrument (one column, MIXED-D from Polymer Laboratories) connected with one refractive index detector from Schambeck SFD Gmbh. All GPC analyses were performed using a polymer–*N*,*N*-dimethylformamide (DMF) solution at a flow rate of 1 mL min^{-1} at 70 °C and calibrated with polystyrene standards. Wide-angle X-ray diffraction (WAXD) measurements were performed at room temperature on a Shimadzu XRD-7000 X-ray diffractometer (40 kV, 20 mA), using graphite- monochromatized Cu Kα radiation. Thermogravimetric analysis (TGA) was conducted with a PerkinElmer Pyris 1 TGA. Experiments were carried out on approximately 6–8 mg film samples heated in flowing nitrogen or air (flow rate: 20 cm^3 min^{-1}) at a heating rate of 20 °C min^{-1}. Dynamic mechanical thermal analysis (DMA) was performed using a DMA 2980, TA Instruments (USA), in a tension mode. Coefficiency of thermal expansion (CTE) and softening temperatures (T_s) are measured on a dilatometer (PerkinElmer TMA 7 instrument). Thermomechanical analysis (TMA) was conducted with a PerkinElmer TMA 7 instrument. The TMA experiments were conducted from 50 to 350 °C at a scan rate of 10 °C min^{-1} with a penetration probe 1.0 mm in diameter under an applied constant load of 10 mN. The softening temperature (T_s) was taken as the onset temperature of probe displacement on the TMA traces. The CTE data were determined in the range 50–200 °C by expansion mode. Ultraviolet-visible (UV-vis) spectra of the polymer films were recorded on HP 8453 UV-visible spectrophotometer. An ellipsometer (SOPRA, GES-5*E*) was used to measure the refractive index (n) and the extinction coefficient (k) of the prepared films in the wavelength range of 150–650 nm. The thickness (h) of the prepared film was also determined simultaneously. An atomic force microscope (AFM, Nanoscope Inc., Model DI 5000) and field emission scanning electron microscopy (FE-SEM, JEOL, JSM-6700F) were used to examine the surface morphology of the coated films. The polymer samples were sputtered with platinum before SEM measurement. The microstructure of the prepared films was examined using a JOEL JEM-1230 transmission electron microscope. The color intensity of the polymers was evaluated by MINOLTA CS-100 colorimeter and converted from Yxy to CIE LAB with hue and chroma values and swatch display from Color Metric Converter WEB.

Results and discussion

Synthesis of polyimide and hybrid materials

The organosoluble polyimide **6FPI** was synthesized by one-step polycondensation and the basic characterizations were summarized in Table S1.† The reaction route for polyimide and titania precursors is shown in Scheme 1, and the reaction compositions are also summarized in Table 1. The flexible, transparent, and homogeneous polyimide–nanocrystalline-titania (**6TPX**) hybrid optical films with different titania contents could be successfully prepared and the appearance of a **6TP50** thick optical hybrid film is shown in Fig. 1.

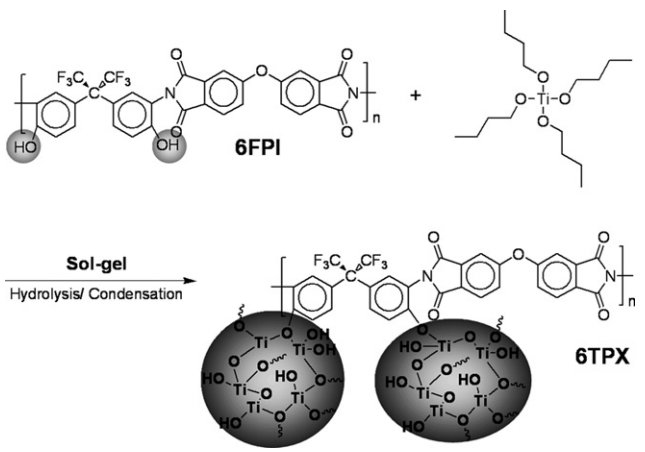

Scheme 1 Hybrid synthesis.

Table 1 Reaction composition and properties of the **6FPI** hybrid films

Sample	Reactant compostition (wt%)		Hybrid film TiO_2 content (wt%)				
	6FPI	$Ti(OBu)_4$	Theoretical	Experimental [a]	h[b]/nm	R_q[c]/nm	n[d]
6FPI	100	0	0	0	156	2.155	1.61
6TP10	67.8	32.2	10	9.9	232	1.859	1.68
6TP30	35.4	64.6	30	28.1	258	2.038	1.73
6TP50	19.0	81.0	50	49.6	635	0.819	1.83
6TP70	9.1	90.9	70	69.8	486	0.397	1.96
TP100	0	100	100	100	132	—	1.99

[a] Experimental titania content estimated from TGA curves. [b] h: Film thickness. [c] R_q: The root mean square roughness. [d] n: Refractive index at 633 nm.

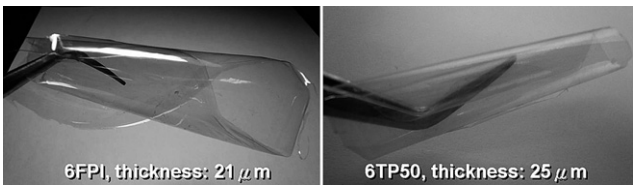

Fig. 1 The photograph shows the appearance of the highly transparent, flexible polyimide and nanocrystalline-titania hybrid optical films.

Properties of polyimide-titania hybrid films

Structural characterizations. The FTIR spectra of **6FPI** and **6TP50** films are shown in Fig. S1.† **6FPI** shows a broad absorption band in the region 3000–3750 cm^{-1} (O–H stretch) and characteristic imide absorption bands at 1771 (asym. C═O str.), 1717 (sym. C═O str.), 1386 (C–N), 1253 (C–F), and 743 cm^{-1} (imide ring deformation), respectively. In Fig. S1(b),† the absorption peak of the polyimide–titania thin film, **6TP50**, at 3000–3750 cm^{-1} is attributed to the hydroxyl groups of the titania crystalline. In addition, the inorganic Ti–O–Ti band is also observed at 650–800 cm^{-1}, which is also similar to that in the previous report.[7]

Thermal properties. The thermal properties of the polyimide–nanocrystalline-titania hybrids were evaluated by TGA, TMA and DMA, and the results were summarized in Table 2. The TGA curves of the hybrid materials in nitrogen and air are shown in Fig. S2 and S3,† respectively, indicated excellent thermal stability of all hybrid materials, and increased carbonized residue (char yield) with increasing titania content. The titania contents in the hybrid materials could be estimated based on the char yields under air flow, which were in good agreement with the theoretical content and ensured successfully incorporation of the nanocrystalline-titania. In addition, an initial 13.7% weight loss of polyimide **6FPI** observed between 370 and 490 °C showed that the expulsion of two molecules of carbon dioxide per repeat unit. The proposed sequence is shown in Scheme S1,† where the hydroxy-imide rearranged to a carboxy-benzoxazole intermediate followed by decarboxylation above 350 °C to give the fully aromatic benzoxazole product.[10] On the other hand, the initial weight loss could not be found in the polyimide–titania hybrid materials, which provided more evidence of completely organic–inorganic bonding.

A typical TMA thermogram for **6TP30** is shown in Fig. S4,† and the softening temperature increased from 190 °C to 370 °C with the increasing titania content. In addition, the dynamic mechanical thermal properties of the polyimide and hybrid films, such as T_g, storage modulus E', and tanδ were also measured and shown in Fig. 2. The dynamic mechanical thermal properties could be enhanced gradually with increasing titania content which restricted the segmental chain mobility by crosslinking between polyimide chains and titania clusters. Meanwhile, **6TP30** also exhibited good damping behavior (tanδ > 0.3) even with a high titania content.

CTE is one of the important designing parameters for the application of polymer films in microelectronic field, the CTE of the pure PI film and the polyimide–nanocrystalline-titania hybrid films were measured and summarized in Table 2. Inorganic reinforced components often revealed much lower

Table 2 Thermal properties of **6FPI** hybrid materials

Polymer	T_g/°C[a]	T_s/°C[b]	CTE (ppm/K)[c]	T_d^5/°C[d]		T_d^{10}/°C[d]		R_{w800} (%)[e]
				N_2	Air	N_2	Air	
6FPI	187	190	93.2	420	445	465	505	51
6TP10	221	203	86.7	480	450	525	510	60
6TP30	309	303	63.2	480	450	525	510	69
6TP50	359	370	49.7	500	455	575	515	80

[a] Glass transition temperature was performed by DMA on PI film specimens (15 mm long, 8 mm wide, and 20–30 μm thick) at a heating rate of 3 °C min^{-1} with a load frequency of 1 Hz in air. [b] Softening temperature measured by TMA with a constant applied load of 10 mN at a heating rate of 10 °C min^{-1} by penetration mode. [c] The CTE data was determined over a 50–200 °C range by expansion mode. [d] Temperature at which 5% and 10% weight loss occurred, respectively, recorded by TGA at a heating rate of 20 °C min^{-1} and a gas flow rate of 30 cm^3 min^{-1}. [e] Residual weight percentages at 800 °C under nitrogen flow.

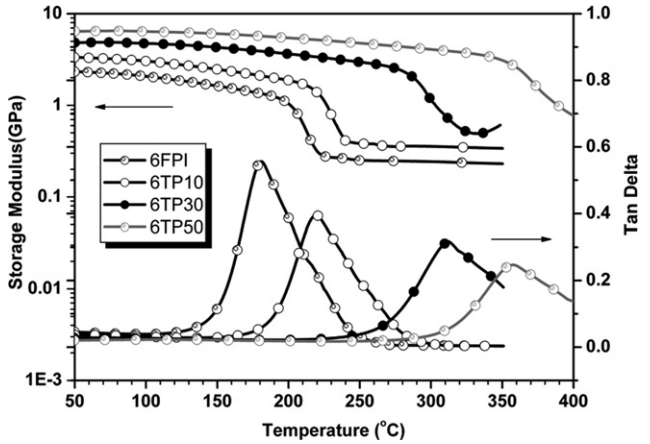

Fig. 2 Storage modulus and tanδ curves of **6FPI** hybrid materials.

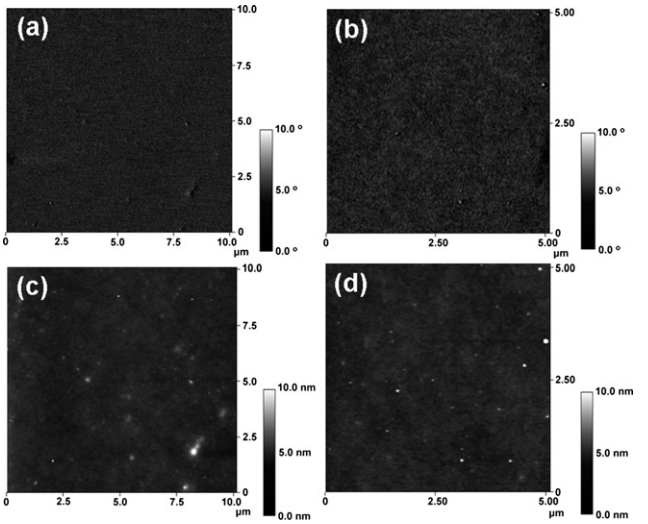

Fig. 4 AFM images of the **6TP50** hybrid films coated on glass: (a) phase images (b) height images; **6TP70** hybrid films coated on glass: (c) phase images (d) height images.

CTE values than that of organic matrixs, which suppressed CTE of the resulting hybrid materials. Therefore, CTE of the organic–inorganic hybrids decrease with increasing the volume fractions of inorganic reinforcement.

Morphology analyses. The SEM images of **6TP50** and **6TP70** films were shown in Fig. 3, which exhibited uniform surface without any apparent microstructural seperation or significant titania aggregates. The height and phase AFM images of **6TP50** and **6TP70** thin films were shown in Fig. 4. The results of root mean square surface roughness (R_q) for the hybrid films analyzed by AFM were listed in Table 1. The ratio of surface roughness to film thickness (R_q/h) was less than 0.15% implying the excellent surface planarity of the hybrid films could be obtained. The results demonstrated that the hydroxyl groups on polyimide played importanct roles for providing the bonding sites with titania thus effectively improving the resultant dispersity and morphology stability of the hybrid materials. Furthermore, the TEM image of the **6TP50** film shown in Fig. 5 exhibited the titania nanocrystallites with the average size of 3–5 nm well dispersed in the hybrid material. The XRD patterns of the hybrid films are shown in Fig. 6, and revealed that the matrix polyimide was amorphous, and the intensity of a titanina crystalline peak gradually increased in the range $2\theta = 23$–27° with increasing titania content suggesting that the titania clusters were well dispersed in polyimides because of hydrolysis-condensation reactions occurred between $Ti(OBu)_4$ and pendant hydroxyl groups of polyimide. The enhanced titania crystallization could be observed obviously in **6TP70**, four peaks, 25.5°, 38.4°, 48.3°, and 54.8°, corresponding to the (101), (112), (200), and (211) crystalline planes of the anatase titania phase, respectively.[11,12] The broad width of the peaks were due to the scattering of X-ray resulted from the small size of the titania nanocrystalline grain. The average crystallite sizes could be estimated to be about 5 nm for **6TP50** by using the Debye–Scherrer equation:

$$B = \frac{0.94 \times \lambda}{d \times \cos\theta} \quad (1)$$

Note that B is the peak's full width at half maximum (FWHM), θ is the peak's position, and d is the average diameter of the crystallite in nanometres.

Optical properties. UV-vis spectra of the **6FPI** hybrid thin films and thick films are shown in Fig. 7. The cutoff wavelengths of the hybrid films in the UV region were contributed to by the chromophores of polyimide, and all the thick hybrid films showed much higher optical transparency than Kapton (Fig. 7(b)). In addition, by increasing the titania content, the intensity of the cutoff wavelengths was enhanced and the

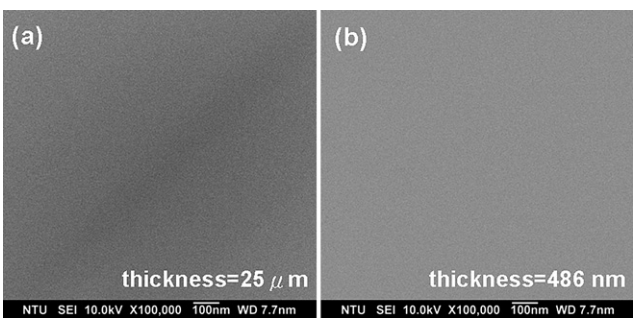

Fig. 3 SEM image of the **6FPI** hybrid materials (a) **6TP50** (film) (b) **6TP70** (coated on glass).

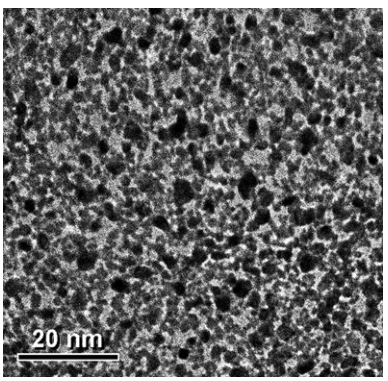

Fig. 5 TEM image of the hybrid material **6TP50**.

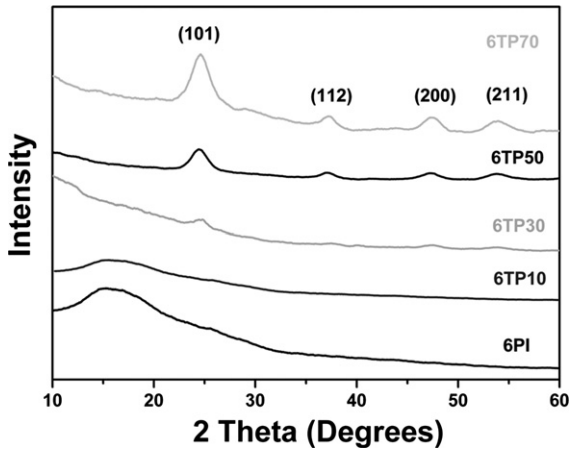

Fig. 6 XRD patterns of the **6FPI** and **6TP10-6TP70** hybrid materials.

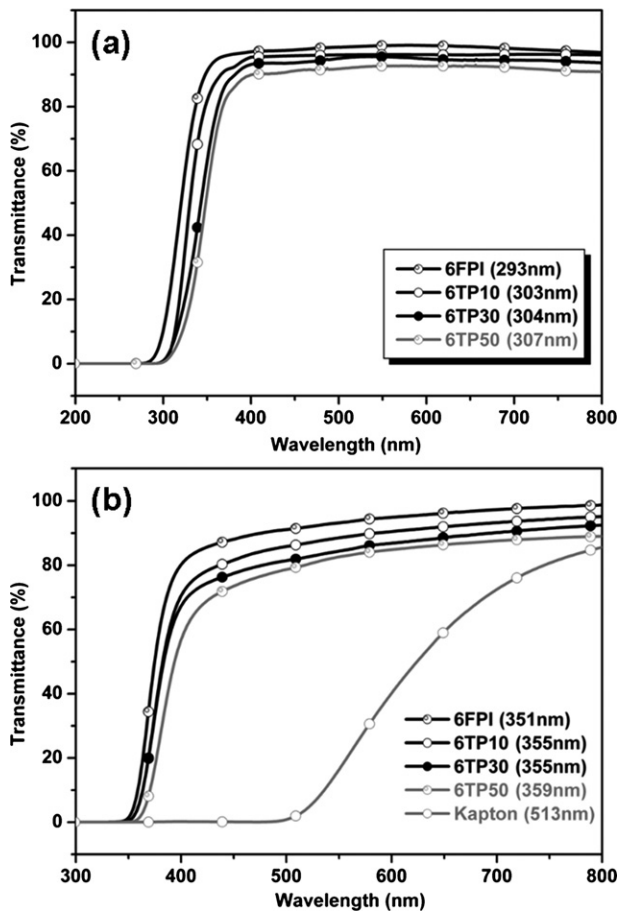

Fig. 7 Transmittance UV-visible spectra of **6FPI** hybrid (a) thin films (thickness: 150–650 nm) and (b) thick films (thickness: 20–30 μm).

corresponding band edge was red-shifted (Table S2†). Such band shift was usually observed for titania sizes less than 10 nm.[7] It indicated that highly homogeneous polyimide–nanocrystalline-titania hybrid materials were obtained, and all the hybrid films showed low cutoff wavelengths and high optical transparency. The light colors of the polyimide-hybrid materials with the bulky and electron-withdrawing CF_3 groups in their diamine moieties could be explained by the decreased CTC formation of polymer chains through higher steric hindrance and lower inductive effect. A secondary positive effect of the CF_3 groups on the film transparency was the weakened intermolecular dispersion forces due to low polarizability of the C–F bond.[13]

The refractive index dispersion of the obtained films at wavelengths of 300–800 nm is shown in Fig. 8, and the insert figure shows the variation of refractive index at 633 nm with titania content. The refractive index increased linearly with increasing titania contents, suggesting that the Ti–OH groups of the hydrolyzed precursors condensed progressively to form the Ti–O–Ti structures and resulted in an enhanced refractive index. It also indicated that using a soluble polyimide with hydroxyl groups on each repeating units is a successful approach for preparing titania hybrid materials. The extinction coefficient of the prepared films shown in Fig. S5† also revealed excellent optical transparency in the visible region, which was agreed with the evaluated color-coordinates of the hybrid films (Table S2†). Combining the issues of thickness, flexibility, and optical transparency, the polyimide–titania hybrid optical thick film **6TP50** (20–30 μm in thickness) showed the best optical transparency with highest titania content and refractive index to the best of our knowledge compared to other polymer–titania hybrid materials.

Multilayer antireflection coatings. The structure of the three-layer anti-reflective coating on the glass substrate and the reflectance spectra are shown in Fig. 9. The glass substrate revealed a refractive index ($n = 1.52$) higher than air ($n = 1.0$) and had an average reflectance of about 4.4% in the visible range. The reflectance could be reduced significantly *via* the three-layer *anti*-reflection coating consisted of **Colloid SiO_2**, **6TP50**, and **6TP10** for the first, second, and third layer, respectively. In order to reduce reflection through adjusting phase of light, the optical thickness (physical thickness × refractive index) was designed to be 0.25 λ_o, 0.5 λ_o, and 0.25 λ_o ($\lambda_o = 550$ nm) for the three-layer structure. Thus, the prepared film thickness and refractive index of **Colloid SiO_2**, **6TP50**, and **6TP10** were 96 nm and 1.29; 150 nm and 1.86; 81 nm and 1.71, respectively. As shown in Fig. 9, the reflectance of prepared anti-reflection coatings was less than 0.7% in the visible range (400 nm to 700 nm), which was

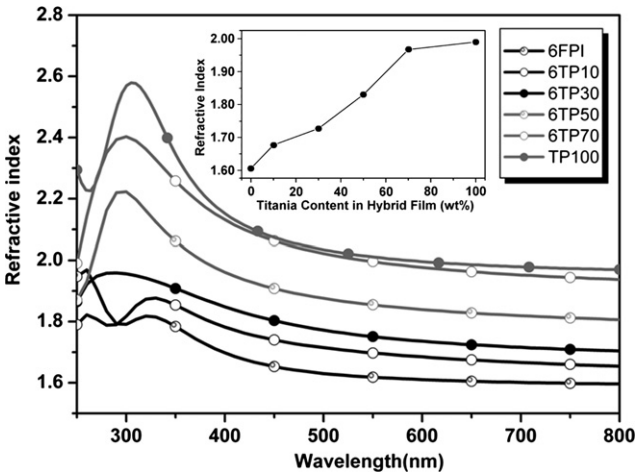

Fig. 8 Variation of the refractive index of the **6FPI** hybrid materials with wavelength. The insert figure shows the variation of refractive index at 633 nm with titania content.

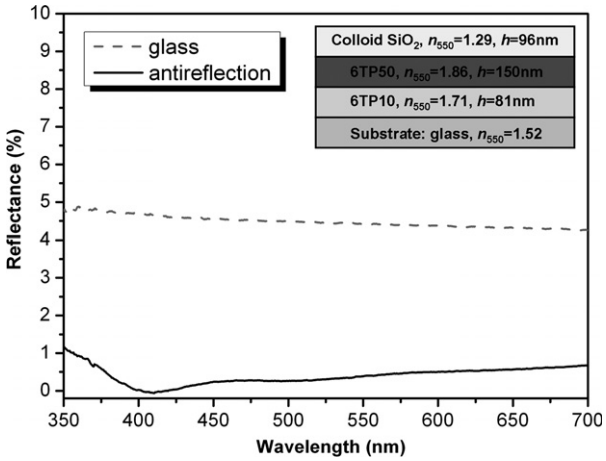

Fig. 9 Variation of the reflectance with wavelength: **BK7** optical glass and the three-layer anti-reflection coating. The insert figure shows the structure of the three-layer anti-reflection coating.

significantly smaller than that of the glass with 4.4%. It suggested the potential application of the prepared polyimide–titania hybrid films in optical devices.

Conclusion

Colorless, transparent, and organosoluble polyimide was readily synthesized from commercial diamine and dianhydride. Furthermore, high transparency and tunable refractive index polyimide–titania hybrid optical films were successfully synthesized from a soluble polyimide with hydroxyl groups and titanium butoxide by controlling the organic : inorganic mole ratio. These hybrid thin films had good surface planarity, high thermal stability, tunable refractive index, low-color and high optical transparency in the visible range. Moreover, the thick titania hybrid films could be achieved even with the relatively high titania content (50 wt%) and refractive index (1.83). To the best of our knowledge, the refractive index and titania content are highest among the highly optical transparent polymer–titania hybrid thick films (20–30 μm in thickness). Three-layer anti-reflective coating based on the hybrid films exhibited reflectance of less than 0.7% in the visible range. It suggested potential optical applications of the novel polyimide–titania hybrid optical films.

Acknowledgements

The authors are grateful to the National Science Council of the Republic of China for financial support of this work.

References and Notes

1 (*a*) L. L. Beecroft and C. K. Ober, *Chem. Mater.*, 1997, **9**, 1302; (*b*) C. Sanchez, B. Lebeau, F. Chaput and J. P. Boilot, *Adv. Mater.*, 2003, **15**, 1969; (*c*) R. M. Laine, *J. Mater. Chem.*, 2005, **15**, 3725; (*d*) A. Zelcer, B. Donnio, C. Bourgogne, F. D. Cukiernik and D. Guillon, *Chem. Mater.*, 2007, **19**, 1992; (*e*) Z. Zhou, A. W. Franz, M. Hartmann, A. Seifert, T. J. J. Muller and W. R. Thiel, *Chem. Mater.*, 2008, **20**, 4986; (*f*) F. Pereira, K. Valle, P. Belleville, A. Morin, S. Lambert and C. Sanchez, *Chem. Mater.*, 2008, **20**, 1710; (*g*) Y. Y. Lin, C. W. Chen, T. H. Chu, W. F. Su, C. C. Lin, C. H. Ku, J. J. Wu and C. H. Chen, *J. Mater. Chem.*, 2007, **17**, 4571.

2 *Functional Hybrid Materials*, ed. P. Gomez-Romero, and C. Sanchez, Wiley-VCH, Weinheim, 2004.

3 G. Kickelbick, *Hybrid Materials: Synthesis, Characterization, and Applications*, Wiley-VCH, Weinheim, 2007.

4 H. Althues, J. Henle and S. Kaskel, *Chem. Soc. Rev.*, 2007, **36**, 1454.

5 (*a*) W. C. Chen, S. J. Lee, L. H. Lee and J. L. Lin, *J. Mater. Chem.*, 1999, **9**, 2999; (*b*) L. H. Lee and W. C. Chen, *Chem. Mater.*, 2001, **13**, 1137; (*c*) A. H. Yuwono, Y. Zhang, J. Wang, X. H. Zhang, H. Fan and W. Ji, *Chem. Mater.*, 2006, **18**, 5876.

6 (*a*) M. Nandi, J. A. Conklin, L. Salvati and A. Sen, *Chem. Mater.*, 1991, **3**, 201; (*b*) C. C. Chang and W. C. Chen, *J. Polym. Sci., Part A: Polym. Chem.*, 2001, **39**, 3419; (*c*) X. L. Guevel, C. Palazzesi, P. Prosposito, G. D. Giustina and G. Brusatin, *J. Mater. Chem.*, 2008, **18**, 3556.

7 H. W. Su and W. C. Chen, *J. Mater. Chem.*, 2008, **18**, 1139.

8 (*a*) B. Wang, G. L. Wilkes, J. C. Hedrick, S. C. Liptak and J. E. McGrath, *Macromolecules*, 1991, **24**, 3449; (*b*) W. C. Chen, L. H. Lee, B. F. Chen and C. T. Yen, *J. Mater. Chem.*, 2002, **12**, 3644; (*c*) S. R. Lu, H. L. Zhang, C. X. Zhao and X. Y. Wang, *Polymer*, 2005, **46**, 10484.

9 J. G. Liu, Y. Nakamura, T. Ogura, Y. Shibasaki, S. Ando and M. Ueda, *Chem. Mater.*, 2008, **20**, 273.

10 D. Likhatchev, C. Gutierrez-Wing, I. Kardash and R. Vera-Graziano, *J. Appl. Polym. Sci.*, 1996, **59**, 725.

11 (*a*) A. H. Yuwono, J. Xue, J. Wang, H. I. Elim, W. Ji, Y. Li and T. J. White, *J. Mater. Chem.*, 2003, **13**, 1475; (*b*) A. H. Yuwono, B. Liu, J. Xue, J. Wang, H. I. Elim, W. Ji, Y. Li and T. J. White, *J. Mater. Chem.*, 2004, **14**, 2978.

12 (*a*) D. Eder and A. H. Windle, *J. Mater. Chem.*, 2008, **18**, 2036; (*b*) M. Miyauchi, *J. Mater. Chem.*, 2008, **18**, 1858; (*c*) A. Yu, G. Q. Lu, J. Drennan and I. R. Gentle, *Adv. Funct. Mater.*, 2007, **17**, 2600; (*d*) D. Fattakhova-Rohlfing, M. Wark, T. Brezesinski, B. M. Smarsly and J. Rathousky, *Adv. Funct. Mater.*, 2007, **17**, 123.

13 W. S. Kim, D. K. Ahn and M. W. Kim, *Macromol. Chem. Phys.*, 2004, **205**, 1932.

